

## Noncovalent Functionalization of Carbon Nanotubes by Fluorescein–Polyethylene Glycol: Supramolecular Conjugates with pH-Dependent Absorbance and Fluorescence

Nozomi Nakayama-Ratchford, Sarunya Bangsaruntip, Xiaoming Sun, Kevin Welsher, and Hongjie Dai\*

Department of Chemistry, Stanford University, Stanford, California 94305

Received December 4, 2006; E-mail: hdai@stanford.edu

Carbon nanotubes are interesting 1D nanomaterials,<sup>1</sup> and to explore nanotubes as macromolecules, various functionalization schemes, both covalent and noncovalent, have been developed to impart water solubility and chemical functionalities.<sup>2</sup> Noncovalent modifications of nanotubes include the use of surfactants and aromatic molecules (e.g., pyrene).<sup>3</sup> Here, we report noncovalent functionalization of single-walled carbon nanotubes (SWNTs) by fluorescein–polyethylene glycol (Fluor-PEG) (**1**) based on a serendipitous observation of strong binding of the molecule on SWNTs. The simple functionalization approach imparts aqueous solubility and simultaneously affords fluorescent labels to nanotubes. Interestingly, the optical absorbance and fluorescence of fluorescein bound to SWNTs are distinctly different from those of free fluorescein, displaying pH-dependent noncovalent binding interactions between molecules and nanotubes. The results are important to the supramolecular chemistry of nanomaterials and potential applications such as pH sensing.

By simple sonication of as-grown SWNTs in an aqueous solution of **1** followed by centrifugation to remove large impurities and dialysis of the supernatant to remove free molecules (see Supporting Information), we obtained SWNTs (average length  $\sim 150$  nm, Figure 1b) stably suspended in water by physisorbed Fluor-PEG (Figure 1c). The hydrophobic aromatic fluorescein group binds to the sidewall of SWNTs (likely via  $\pi$ -stacking) while the PEG group extends into water. The nanotube suspension was stable in water without aggregation even after heating to 70 °C for 2 days (Figure 1c). High stability was also observed in cell culture medium containing 10% fetal bovine serum and  $\sim 150$  mM salt (Figure 1c), suggesting strong binding of Fluor-PEG on SWNTs.

We investigated the optical absorbance and fluorescence characteristics of fluorescein bound to SWNTs in phosphate buffered saline (PBS) at pH 7.4 (note: free unbound fluorescein in all of our SWNT suspensions were removed by dialysis). UV–vis–NIR spectra clearly revealed an absorbance peak (at  $\sim 497$  nm) of fluorescein bound to SWNTs (Figure 2a in which the background spectrum with small peaks was due to SWNTs), and the peak was red-shifted (by  $\sim 3$  nm) relative to free fluorescein. The number of Fluor-PEG per tube (average length  $\sim 150$  nm) was estimated to be  $\sim 90$  with a  $\sim 12\%$  coverage of the SWNT sidewall area (see Supporting Information Figure S1). We observed  $\sim 67\%$  quenching of the fluorescence of SWNT-bound fluorescein relative to free fluorescein at the same concentration (495-nm excitation) (Figure 2b) due to interactions between fluorescein and SWNT. Similar fluorescence quenching was reported for SWNT-bound pyrene due to energy transfer.<sup>4,5</sup> The  $\sim 67\%$  quenching effect was observed for various SWNT concentrations up to 10 nM with fluorescein concentrations up to  $\sim 900$  nM (Figure 2c).

The absorbance (at 490 nm) and fluorescence of fluorescein are known to increase at higher pHs under higher degrees of deprotonation and saturate around pH  $\approx 8$ .<sup>6–8</sup> Although a similar trend

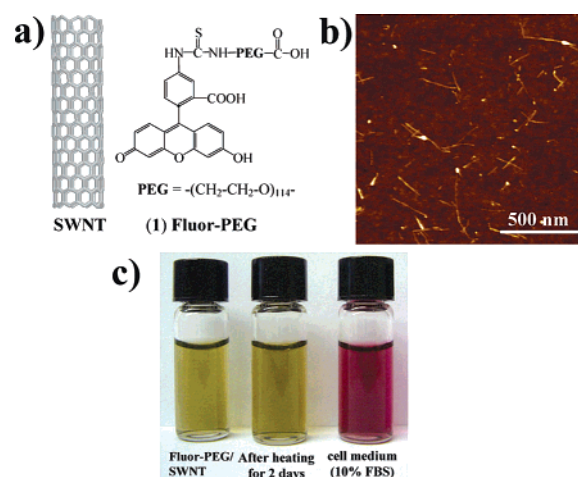


**Figure 1.** Fluor-PEG-functionalized SWNTs. (a) Schematic showing SWNT and Fluor-PEG (**1**). (b) Atomic force microscopy image of Fluor-PEG/SWNTs deposited on substrate. (c) Photo of Fluor-PEG/SWNT in water (left, yellow-green color due to SWNT-bound Fluor), after heating at 70 °C for 2 days (center), and in cell culture medium supplemented with 10% serum (right, red color due to cell medium). Unbound Fluor-PEG was dialyzed in the starting solution.

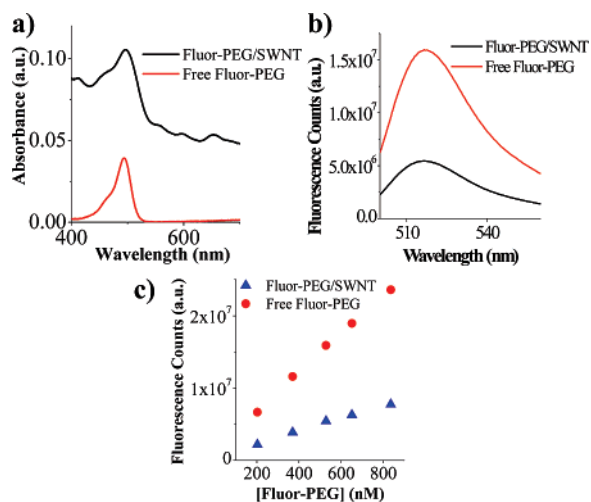


**Figure 2.** Optical properties of SWNT-bound Fluor-PEG. (a) Absorbance of Fluor-PEG/SWNT and free Fluor-PEG. (b) Corresponding fluorescence emission spectra. (c) Emission peak intensity of SWNT bound Fluor-PEG and free Fluor-PEG in a fluorescein concentration range of 200–900 nM.

was observed for fluorescein bound to SWNTs under increasing pH, no saturation was seen even up to pH  $\approx 12$  (Figure 3a,c,d). No significant pH dependence was observed in the absorbance (Figure 3b) and photoluminescence (Figure S3) of our SWNTs, in contrast with SWNTs solubilized by surfactants with charged groups and without PEGylation.<sup>9,10</sup> This difference is currently not

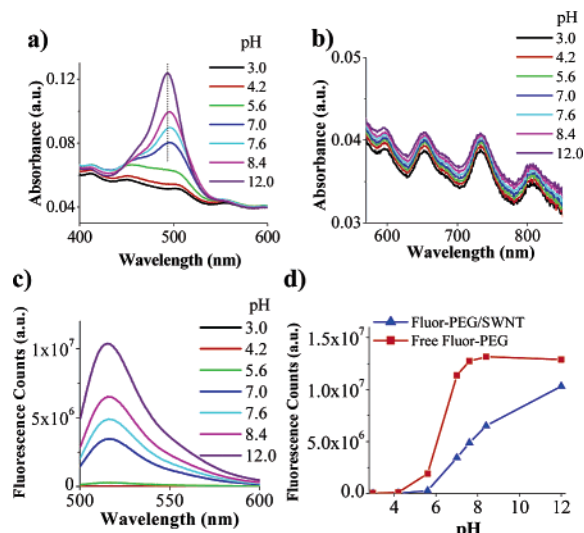


**Figure 3.** pH-dependent fluorescence and absorbance of Fluor-PEG/SWNT. Absorption curves of Fluor-PEG/SWNT at various pHs in the (a) fluorescence region (dashed line marks the peak at  $\text{pH} \approx 12$ ) and (b) SWNT region (curves are displaced for clarity). (c) Corresponding fluorescence emission spectra ( $\lambda_{\text{excitation}} = 495 \text{ nm}$ ). (d) Comparison of emission peak intensity dependence on pH of free Fluor-PEG and Fluor-PEG/SWNT with the same Fluor-PEG concentration.

understood but could be due to the different functionalization schemes used. The absorbance peaks of SWNT-bound fluorescein exhibited monotonic blue-shift (Figure 3a) at higher pHs, approaching the characteristics of free fluorescein (i.e., reversing the effects of fluorescein–SWNT binding). This suggested that the increase in pH led to weakening of the interaction between fluorescein and SWNT, reducing fluorescence quenching, and shifting the spectral peaks back to near that of free fluorescein. At pH 12, we observed slow but noticeable precipitation of Fluor-PEG/SWNTs from the solution after standing for  $\sim 48 \text{ h}$  while no precipitates were seen in lower pH solutions (see Supporting Information, Fig. S 2). This confirmed weakened interaction between fluorescein and SWNT at higher pHs, causing Fluor-PEG desorption over time. The mechanism of reduced interaction at higher pHs is not yet fully understood, but we speculate that higher pH and deprotonation impart higher hydrophilicity to fluorescein and thus higher affinity for water solvation. The monotonic increase of Fluor-PEG/SWNT fluorescence without saturation at  $\text{pH} \sim 8$  expected for free fluorescein could also be due to delayed deprotonation of fluorescein when bound to SWNT, or competition of hydroxyl ion with (1) for SWNT binding, though further work is needed to fully understand the various possible mechanisms.

Our simple functionalization imparts solubility to nanotubes in physiological buffers and simultaneously affords fluorescent labels. The fluorescence intensity of fluorescein on SWNT is  $\sim 33\%$  of free fluorescein, which can still be utilized in chemical and biological settings. To this end, we investigated the cellular uptake of Fluor-PEG/SWNT and used fluorescence detections for characterization. After incubation of BT474 breast cancer cells in a solution of Fluor-PEG/SWNT, we observed fluorescein signals within cells by confocal fluorescence microscopy (Figure 4a) and flow cytometry (or fluorescence activated cell sorting (FACS), Figure 4b). Further, owing to the strong resonance Raman signatures of SWNTs, we used the G-band Raman peak at  $\sim 1600 \text{ cm}^{-1}$ , characteristic of graphitic stretching mode, to directly probe SWNTs in live cells. A micro-Raman image formed by spatially mapping out the G-band-integrated intensity showed the existence of SWNTs at the cells (Figure 4c,d), and the co-localization with fluorescein

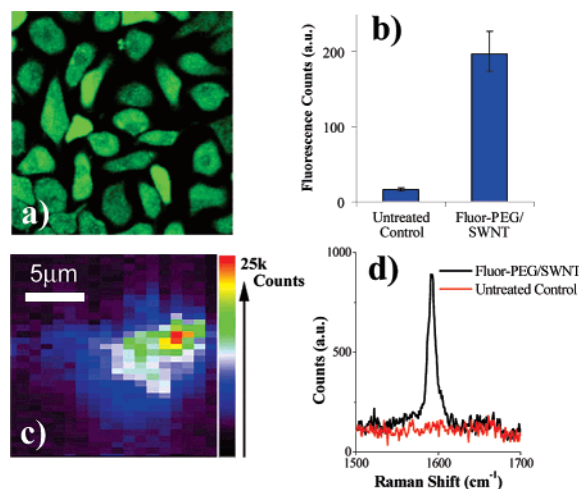


**Figure 4.** Cellular uptake of Fluor-PEG/SWNT. (a) Confocal fluorescence image of BT474 cells incubated with Fluor-PEG/SWNT. (b) Fluorescence intensities of large population of cells treated with Fluor-PEG/SWNT vs untreated control cells by flow cytometry. (c) Micro-Raman image of the cells incubated with Fluor-PEG/SWNT. (d) Representative Raman spectra showing the presence and absence of the SWNT G-band from Fluor-PEG/SWNT-incubated cells and untreated control cells, respectively.

fluorescence suggested the cellular uptake of Fluor/SWNT conjugates, similar to internalization of other molecular complexes with nanotubes.<sup>11,12</sup> Control cells without exposure to Fluor-PEG/SWNT showed minimal fluorescence and SWNT G-band Raman signal (Figure 4b,d).

We have used PEGylated fluorescein to noncovalently functionalize SWNTs to obtain aqueous stable conjugates with pH-dependent optical properties. We showed that the finite fluorescence intensity of fluorescein-PEG/SWNT can be utilized for detection, imaging and cell sorting in biological applications. Last, since the terminal group of Fluor-PEG on the SWNT conjugate is a carboxylic acid (Figure 1a), one can envision conjugation of various molecules to the conjugates to impart further chemical or biological functionalities.

**Acknowledgment.** This work was partly supported by NIH-NCI CCNE-TR and a Stanford Translational Research Grant.

**Supporting Information Available:** Experimental details. This material is available free of charge via the Internet at <http://pubs.acs.org>.

## References

- (1) Dresselhaus, M. S.; Dresselhaus, G.; Eklund, P. C. *Science of Fullerenes and Carbon Nanotubes*; Academic Press: San Diego, 1996; pp 1–985.
- (2) Britz, D. A.; Khlobystov, A. N. *Chem. Soc. Rev.* **2006**, *35*, 637.
- (3) Chen, R. J.; Zhan, Y. G.; Wang, D. W.; Dai, H. J. *J. Am. Chem. Soc.* **2001**, *123*, 3838.
- (4) Tomonari, Y.; Murakami, H.; Nakashima, N. *Chem. Eur. J.* **2006**, *12*, 4027.
- (5) Paloniemi, H.; Aaritalo, T.; Laiho, T.; Liuke, H.; Kocharova, N.; Haapakka, K.; Terzi, F.; Seiber, R.; Lukkari, J. *J. Phys. Chem. B* **2005**, *109*, 8634.
- (6) Invitrogen Molecular Probes. In *The Handbook: A Guide to Fluorescent Probes and Labeling Technologies*. Web Edition, accessed 11/2006; Section 20.2.
- (7) Diehl, H. *Talanta* **1989**, *36*, 413.
- (8) Diehl, H.; Markuszewski, R. *Talanta* **1989**, *36*, 416.
- (9) Strano, M. S.; Huffman, C. B.; Moore, V. C.; O'Connell, M. J.; Haroz, E. H.; Hubbard, J.; Miller, M.; Rialon, K.; Kittrell, C.; Ramesh, S.; Hauge, R. H.; Smalley, R. E. *J. Phys. Chem. B* **2003**, *107*, 6979.
- (10) Dukovic, G.; White, B.; Zhou, Z.; Wang, F.; Jockusch, S.; Steigerwald, M.; Heinz, T.; Friesner, R.; Turro, N. J.; Brus, L. E. *J. Am. Chem. Soc.* **2004**, *126*, 15269.
- (11) Kam, N. W. S.; Liu, Z.; Dai, H. J. *J. Am. Chem. Soc.* **2005**, *127*, 12492.
- (12) Kam, N. W. S.; Jessop, T. C.; Wender, P. A.; Dai, H. J. *J. Am. Chem. Soc.* **2004**, *126*, 6850.

JA068684J

**Noncovalent Functionalization of Carbon Nanotubes by Fluorescein-Polyethylene Glycol: Supramolecular Conjugates with pH Dependent Absorbance and Fluorescence**

Nozomi Nakayama-Ratchford, Sarunya Bangsaruntip, Xiaoming Sun,  
Kevin Welsher, and Hongjie Dai\*

*Department of Chemistry, Stanford University, Stanford, California 94305*

**Supplementary Information with Supplementary Figures**

**Functionalization of SWNTs by Fluorescein-PEG-COOH.**

1 mM of fluorescein-PEG-NHS (PEG MW 5000 Da, Nektar Therapeutics) was sonicated with 0.25 mg/mL of HiPco SWNTs (Carbon Nanotechnologies Inc) in water for ~0.5-1h, and the resulting dark suspension was centrifuged at 25,000 g for 6 hrs. The pellet formed at the bottom of the centrifuge tube containing aggregates such as bundles and impurities was discarded. The supernatant was collected and filtered through a centrifugal filter device (100k Da MWCO, Millipore Amicon) to remove excess pegylated fluorescein, washed with water several times, and re-suspended in water. The solution was subsequently dialyzed (1 M Da MWCO, SpectrumLabs Spectra/Por Biotech CE membrane) over a few days to ensure complete excess removal. Note that the NHS group of the fluorescein-PEG-NHS hydrolyzes over the preparation period and becomes a carboxyl group in the final product.

**Characterization of Fluor-PEG/SWNT.**

Atomic Force Microscopy (AFM). Fluor-PEG/SWNT was deposited on SiO<sub>2</sub> by soaking a piece of SiO<sub>2</sub> in the Fluor-PEG/SWNT solution in 10 mM HCl for ~15 min. The acid neutralizes the charge on Fluor-PEG and helps the Fluor-PEG/SWNT conjugate to adsorb on SiO<sub>2</sub>. The SiO<sub>2</sub> substrate was rinsed briefly with water, blow dried with air, and used for AFM imaging. Lengths of 100 SWNTs were measured, and the average length was estimated to be ~158 nm.

UV-vis-NIR Spectroscopy. UV-vis-NIR measurement was carried out using Cary 6000i spectrophotometer. The nanotube concentration in Fluor-PEG/SWNT solution was estimated by the absorbance value at 808 nm and using the extinction coefficient  $7.9 \times 10^6 \text{ M}^{-1} \text{ cm}^{-1}$  (assumes ~150 nm 170k Da SWNTs).<sup>1</sup> The path length used for the measurements was 1 cm. The absorption spectrum of the nanotube solution shows distinct peaks in the UV-vis-NIR region, characteristic of highly dispersed individualized SWNTs.

Stability. The aqueous stability of Fluor-PEG/SWNT at high temperature and in high salt and protein environment was assessed by the following: 25 nM of Fluor-PEG/SWNT in water was heated to 70 °C for 2 days. A small volume of a concentrated Fluor-PEG/SWNT solution was added to cell culture medium (Dulbecco's Modified Eagle's Medium, Invitrogen) with 10% fetal bovine serum (FBS) such that the final concentration of Fluor-PEG/SWNT was 25 nM. Fluor-PEG/SWNT remained soluble in both cases and no aggregation was observed, even after a centrifugation step at 2000 g for 10 min.

---

<sup>1</sup> Kam, N. W. S.; O'Connell, M.; Wisdom, J. A.; Dai, H. J. *PNAS* **2005**, *102*, 11600.

Estimation of Number of Fluor-PEG per SWNT. To determine the amount of Fluor-PEG adsorbed on SWNT, a high concentration of another surfactant known to be efficient at adsorbing and solubilizing SWNT in water was added to Fluor-PEG/SWNT solution to displace the Fluor-PEG adsorbed on SWNT. 1 mg/mL ( $\sim 360 \mu\text{M}$ ) of 1,2-Distearoyl-*sn*-Glycero-3-Phosphoethanolamine-N-[Amino(Polyethylene Glycol)2000] (PL-PEG-NH<sub>2</sub>, Avanti Polar Lipids)<sup>2</sup> was added to Fluor-PEG/SWNT solution with the following 5 concentrations of nanotubes: 2.0, 3.2, 4.8, 6.6, and 7.8 nM. (Note: Fluor-PEG/SWNT suspension used was after removal of excess Fluor-PEG by dialysis to prevent excess Fluor-PEG from contributing to the fluorescence signal.) It was allowed to react overnight followed by 10 min sonication. Emission spectrum of the resulting solutions containing freed Fluor-PEG and PL-PEG-NH<sub>2</sub>/SWNT in 1 mg/mL of PL-PEG-NH<sub>2</sub> at the 5 different SWNT concentrations was measured with a spectrofluorometer ( $\lambda_{\text{excitation}} = 495 \text{ nm}$ ,  $\lambda_{\text{emission}}$  scanned from 500-600 nm, Spex Fluorolog 3). To determine the concentration of this freed Fluor-PEG, calibration curve of Fluor-PEG fluorescence intensity was obtained by adding known concentrations of Fluor-PEG to a background of 5 nM of PL-PEG-NH<sub>2</sub>/SWNT in 1 mg/mL of PL-PEG-NH<sub>2</sub>. The concentrations of freed Fluor-PEG, which is the concentration of Fluor-PEG adsorbed on SWNTs, are plotted against the corresponding Fluor-PEG/SWNT concentration in S fig. 1. The number of Fluor-PEG attached to each SWNT was estimated and is also plotted. Fluor-PEG concentration increased linearly with SWNT concentration in the range of 1-5 nM, and correspondingly, the number of Fluor-PEG per SWNT remained constant in this range at an average of  $\sim 88$  Fluor-PEG per SWNT. This value can be more accurately described

---

<sup>2</sup> Kam, N. W. S.; Liu, Z.; Dai, H. J. *J. Am. Chem. Soc.* **2005**, *127*, 12492.

as 11  $\mu\text{M}$  of Fluor-PEG per absorption unit at 808 nm (or 0.5  $\mu\text{mol}$ s Fluor-PEG per 1 mg of SWNT) since this does not make any assumptions on the molar extinction coefficient.

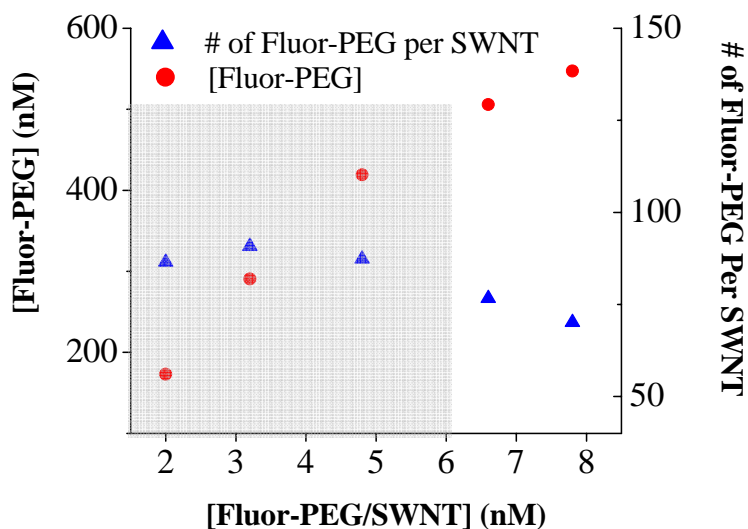


**Figure S1.** Plot of concentration of free fluor-PEG detached from the SWNT as a function of concentration of SWNT (red dots) and the number of fluor attached on each SWNT (blue triangle). The gray box indicates the linear region that was used to obtain the average number of fluor per SWNT,  $\sim 90$ .

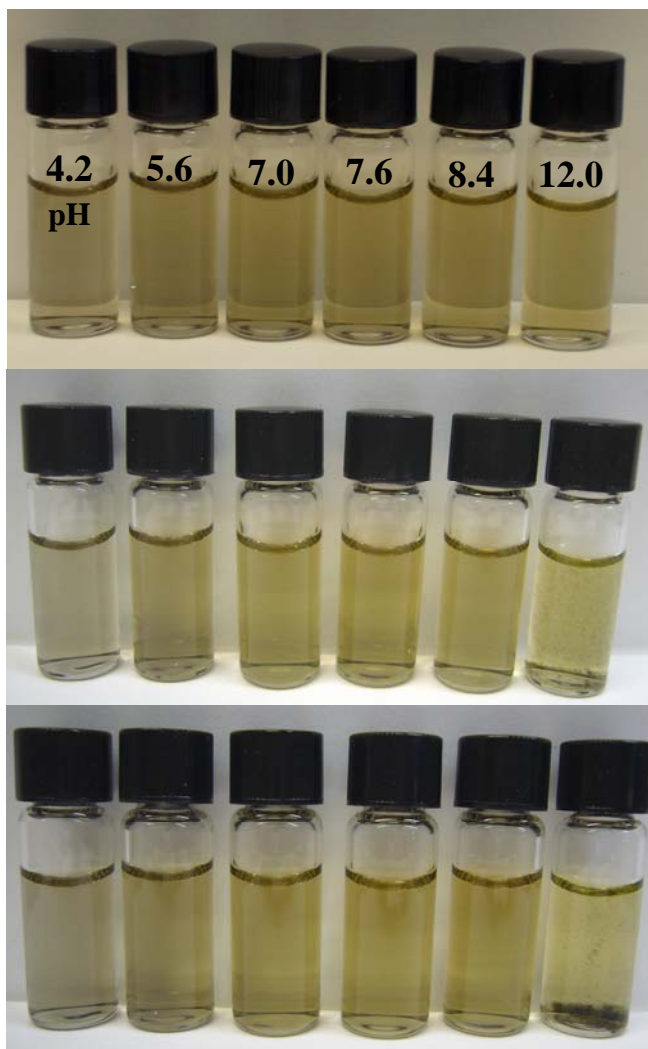
Estimation of SWNT coverage by Fluor-PEG. Using 170k Da as the molar mass of a  $\sim 150\text{nm}$  long SWNT, the number of carbons per SWNT was calculated to be  $170\text{kg/mole} \div 12\text{g/mole} = 1.4 \times 10^4$ . If we assume that all the atoms in the ring system of fluorescein are interacting with the SWNT via  $\pi$ -stacking, there are 20 atoms interacting with the SWNT aromatic rings. Since there are  $\sim 88$  fluor attached to each tube,  $20 \text{ atoms/fluor} \times 88 \text{ fluor/SWNT} = 1760$  carbon atoms of a SWNT are being covered by the adsorbed fluor. This corresponds to  $\sim 12\%$  coverage ( $1760 \div 1.4 \times 10^4 = 0.12$ ).

### Fluorescence and Absorbance Properties of SWNT bound Fluorescein.

Emission and absorption spectrum of Fluor-PEG/SWNT suspension in phosphate buffered saline (PBS) at pH 7.4 (Invitrogen) was measured at the following 5 concentrations ( $\lambda_{\text{excitation}} = 495 \text{ nm}$ ): 2.3, 4.2, 6.0, 7.4, and 9.5 nM. Using  $\sim 88$  Fluor-PEG per SWNT, the corresponding Fluor-PEG concentration attached to the SWNT at the 5 concentrations was calculated to be 202, 370, 528, 651, and 836 nM, and free Fluor-PEG solutions at these concentrations were prepared in PBS. The emission spectra of these free Fluor-PEG solutions in PBS were measured for comparison. The absorption and emission curves for 6.0 nM Fluor-PEG/SWNT and 528 nM Fluor-PEG are shown in Fig. 2a and b respectively. The plot of the fluorescence intensity at 517 nm of Fluor-PEG/SWNT and Fluor-PEG with respect to Fluor-PEG concentration is shown in Fig. 2c. The fluorescence intensity of Fluor-PEG/SWNT at 517 nm is  $\sim 33\%$  that of free Fluor-PEG at all 5 concentrations of Fluor-PEG.

pH Dependence of SWNT bound Fluorescein Emission and Absorption. 4.6 nM Fluor-PEG/SWNT solutions at various pHs were prepared in 10 mM phosphate buffer with 150 mM NaCl at pHs: 3.0, 4.2, 5.6, 7.0, 7.6, 8.4, and 12. The absorption and emission ( $\lambda_{\text{excitation}} = 495 \text{ nm}$ ) spectra of each solution were measured (Fig. 3a and b). For comparison, 405 nM ( $88 \times 4.6 = 405 \text{ nM}$ ) Fluor-PEG solutions at the same pHs were also prepared, and the emission spectra of these solutions were measured. The emission peak intensity (at 517 nm) of Fluor-PEG/SWNT and free fluor as a function of pH is plotted in fig. 3c.

pH Dependence of Aqueous Stability of Fluor-PEG/SWNT. Fluor-PEG/SWNT solutions at different pHs were prepared at the same concentration and observed over several days for precipitates.



Day 1  
No precipitation is observed.

Day 4  
After >48hs, we can start to see black precipitates from the pH 12 solution.

Day 5  
SWNT precipitates have settled at the bottom from the pH 12 solution, but more are still precipitating out. No precipitates were observed for the lower pHs.

**Figure S2.** Photographs of Fluor-PEG/SWNT solutions (with same nanotube concentration) at various pHs recorded after standing for various times indicated. Precipitation of nanotubes was seen in the pH 12 solution but not in the others.

Fluor-PEG/SWNTs are less stable at high pHs, suggesting weaker interaction between SWNT and Fluor-PEG. Fluor-PEG desorbs slowly from the SWNT surface over time.

pH Dependence of SWNT Photoluminescence of SWNTs solubilized by Fluor-PEG. We have measured the pH dependence of SWNT photoluminescence in the near IR using an InGaAs detector at 785nm laser excitation. We observed no significant pH dependence in the pH range studied as shown in Fig.S3, which differed from the results in ref. 9 and 10. This difference was currently not understood, but could be related to the different coatings on the nanotubes (neutral PEGylation in our case and surfactants with charged groups in other cases). That is, the response of SWNT photoluminescence emission to pH could depend on the type of functionalization. Future work is needed to reconcile the different observations.

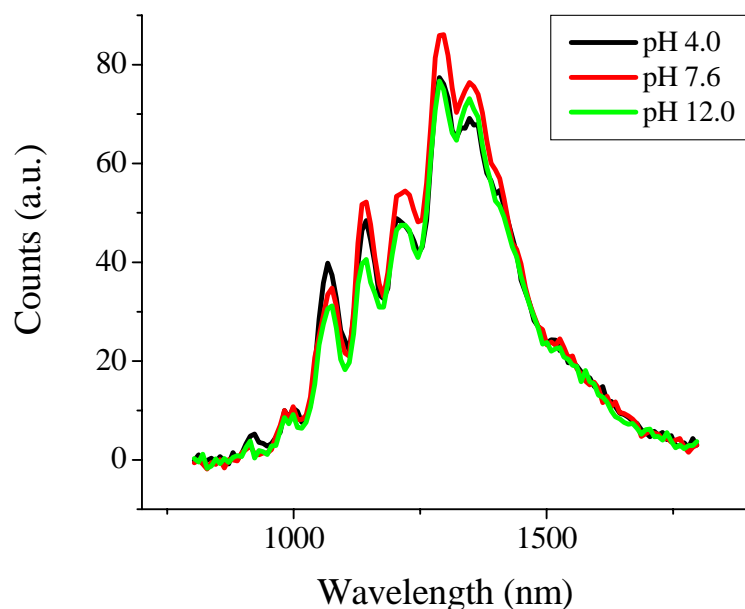


**Figure S3.** NIR photoluminescence spectra of Fluor-PEG/SWNT solutions (with same nanotube concentration) in phosphate buffers at the various pHs.

**Internalization of Fluor-PEG/SWNT by mammalian cells.**

Incubation of Fluor-PEG/SWNT with BT474 Cells. A breast cancer cell line, BT474, was grown in cell culture medium (Dulbecco's Modified Eagle's Medium, Invitrogen) supplemented with 10% FBS. Prior to incubation, the cells were collected by centrifugation and resuspended in the culture medium at a cell density of  $\sim 1 \times 10^6$  cells/mL. 200  $\mu$ L of the cell suspension was mixed with 50  $\mu$ L of a 500 nM Fluor-PEG/SWNT solution. The cells were incubated in the Fluor-PEG/SWNT solution for 24 h at 37°C, in 5% CO<sub>2</sub> atmosphere.

Confocal Microscopy Imaging of Cells. After the incubation step above, the BT474 cells were washed twice with fresh cell medium to remove uninternalized Fluor-PEG/SWNT, then immediately imaged in chambered cover slides by Zeiss LSM 510 confocal fluorescence microscope.

Flow Cytometry. Also after incubation, the cells were washed to remove excess Fluor-PEG/SWNT, detached by trypsin-EDTA (Gibco), collected by centrifugation and re-suspended in cell culture medium. The cells were analyzed by a Becton-Dickinson FACScan instrument. 2% propidium iodide (PI, Fluka chemicals) was added to the cell suspension prior to the measurement. PI is a membrane impermeable dye and does not stain live cells. It can enter dead cells and intercalate into DNA, thereby selectively staining the dead cells. We carried out dual detection of red (PI) and green fluorescence (fluorescein) with the cells. The data presented here represent the mean green (fluorescein) fluorescence obtained with a population of 6, 000 live cells.

Micro-Raman Mapping of Incubated Cells. After incubation in 48-well culture plates (250  $\mu$ l cell medium in each well) for 24 h, the cells were washed twice to remove

uninternalized Fluor-PEG/SWNT, detached by trypsin-EDTA (Gibco), collected by centrifugation and re-suspended in 50  $\mu\text{l}$  cell culture medium. 10  $\mu\text{l}$  of the cell suspension was dropped on a thin plastic film and covered by another thin plastic film. The scanning area was selected by focusing on the cells using the microscope, and the micro-Raman laser was then focused at this plane ( $\lambda_{\text{excitation}} = 785 \text{ nm}$ ). A line scanning mode was applied to get a Raman spectrum at every point in the selected area ( $1 \mu\text{m} \times 1 \mu\text{m}$  for each point). The image was obtained by plotting the integrated area in the range  $1580\text{-}1610 \text{ cm}^{-1}$  of the Raman spectra obtained in the cell area.

A Raman image of the cells incubated with Fluor-PEG/SWNT is shown in figure 4c. While the presence of the G-band signal from the cells does not directly show that SWNTs are inside of the cells, this shows that SWNTs are present at the cells and suggests that Fluor-PEG/SWNTs are inside because SWNTs and Fluor-PEG are attached, and the fluorescein fluorescence was shown to be coming from the inside. Control cells without Fluor-PEG/SWNT have no G-band signal showing that cells do not have contributing peaks at  $1600 \text{ cm}^{-1}$  (data not shown).